Autophagy 8:7, 1098–1112; July 2012; © 2012 Landes Bioscience

MAPK14/p38α confers irinotecan resistance to TP53-defective cells by inducing survival autophagy

Salomé Paillas,[1] Annick Causse,[1] Laetitia Marzi,[1] Philippe De Medina,[2] Marc Poirot,[2] Vincent Denis,[1] Nadia Vezzio-Vie,[1] Lucile Espert,[3] Hayat Arzouk,[1] Arnaud Coquelle,[1] Pierre Martineau,[1] Maguy Del Rio,[1] Sophie Pattingre[1] and Céline Gongora[1,*]

[1]Institut de Recherche en Cancérologie de Montpellier (IRCM); Montpellier, France; INSERM; U896; Montpellier, France; Université Montpellier1; Montpellier, France; CRLC Val d'Aurelle Paul Lamarque; Montpellier, France; [2]Inserm U563; Toulouse, Haute-Garonne, France; [3]CPBS; UMR5236; CNRS/UMI-UMII; Montpellier, France

Keywords: MAPK14/p38, survival autophagy, irinotecan resistance, colon cancer, chemotherapy

Abbreviations: ATG, autophagy-related; Baf, bafilomycin A_1; CRC, colorectal cancer; EGFR, epidermal growth factor receptor; FOLFIRI, 5-fluorouracil/leucovorin and irinotecan; FOLFOX, 5-fluorouracil/leucovorin and oxaliplatin; HCT116-TP53KO, HCT116 human colorectal adenocarcinoma cells in which *TP53* was genetically ablated; HCT116-TP53KO-MAPK14-CA cells, HCT116-TP53KO cells in which constitutively active p38alpha (MAPK14) was stably transduced; HCT116-TP53KO-EV cells, HCT116-TP53KO cells stably transduced with an empty vector (pMSCV) to serve as a control; HCT116-MAPK14-CA cells, HCT116 cells in which constitutively active p38alpha (MAPK14) was stably transduced; HCT116-EV cells, HCT116 cells stably transduced with an empty vector (pMSCV) to serve as a control; HCT116-TP53KO-ShMAPK14, HCT116-TP53KO cells in which Shp38alpha (MAPK14) was stably transduced; HCT116-TP53KO-ShLuc, HCT116-TP53KO cells in which ShpLuc was stably transduced to serve as a control; LC3, microtubule-associated protein 1 light chain 3; 3MA, 3-methyladenine; MAPK, mitogen-activated protein kinase; MAPK14, p38 alpha; MAPK11, p38 beta; MAPK12, p38 gamma; MAPK13, p38 delta; NT, untreated cells; p38α, MAPK p38 alpha (MAPK14); FAM48A, p38 interacting protein (p38IP); PtdIns3K, phosphatidylinositol 3-kinase; SRB assays, sulforhodamin B assay; SN38, active metabolite of irinotecan; ShLuc, shRNA targeting luciferase, serve as a control; ShMAPK14, shRNA targeting p38α (MAPK14); siCT, control siRNAs; TOP1, topoisomerase I; VEGF, vascular endothelial growth factor

Recently we have shown that the mitogen-activated protein kinase (MAPK) MAPK14/p38α is involved in resistance of colon cancer cells to camptothecin-related drugs. Here we further investigated the cellular mechanisms involved in such drug resistance and showed that, in HCT116 human colorectal adenocarcinoma cells in which *TP53* was genetically ablated (HCT116-TP53KO), overexpression of constitutively active MAPK14/p38α decreases cell sensitivity to SN-38 (the active metabolite of irinotecan), inhibits cell proliferation and induces survival-autophagy. Since autophagy is known to facilitate cancer cell resistance to chemotherapy and radiation treatment, we then investigated the relationship between MAPK14/p38α, autophagy and resistance to irinotecan. We demonstrated that induction of autophagy by SN38 is dependent on MAPK14/p38α activation. Finally, we showed that inhibition of MAPK14/p38α or autophagy both sensitizes HCT116-TP53KO cells to drug therapy. Our data proved that the two effects are interrelated, since the role of autophagy in drug resistance required the MAPK14/p38α. Our results highlight the existence of a new mechanism of resistance to camptothecin-related drugs: upon SN38 induction, MAPK14/p38α is activated and triggers survival-promoting autophagy to protect tumor cells against the cytotoxic effects of the drug. Colon cancer cells could thus be sensitized to drug therapy by inhibiting either MAPK14/p38 or autophagy.

Introduction

Colorectal cancer (CRC) is the third most frequent malignancy in Western countries. The current chemotherapy options for patients with metastatic CRC include the combination of 5-fluorouracil/leucovorin and irinotecan (FOLFIRI), or of 5-fluorouracil/leucovorin and oxaliplatin (FOLFOX) associated, or not, with the anti-VEGF antibody Bevacizumab or the anti-EGFR antibody Cetuximab.[1] Treatment with Cetuximab is restricted to patients with wild-type *KRAS*, because *KRAS* mutations predict resistance to treatment with anti-EGFR monoclonal antibodies.[2] As therapeutic failure is mainly due to resistance to drug treatment, identifying the cellular mechanisms that lead to such resistance is a crucial issue for improving the management and survival of patients with CRC.

*Correspondence to: Céline Gongora; Email: celine.gongora@inserm.fr
Submitted: 09/28/12; Revised: 04/03/12; Accepted: 04/04/12
http://dx.doi.org/10.4161/auto.20268

SN38 is the active metabolite of irinotecan (CPT-11), a derivative of camptothecin. Like other camptothecin-derivatives, SN38 inhibits topoisomerase I (TOP1), a nuclear enzyme needed for replication and transcription by unwinding supercoiled DNA.[3] SN38 interferes with TOP1 activity by trapping TOP1-DNA cleavage complexes, leading to lethal replication-mediated, double-strand breaks.[3] Cellular mechanisms causing irinotecan resistance have been identified for each step of the CPT-11 pathway.[4] We previously showed that SN38-resistant HCT116 cells display endogenous activation of the mitogen-activated protein kinase (MAPK) p38.[5] Specifically, p38 is activated by treatment with SN38 and pharmacological inhibition of MAPK14/p38α and MAPK11/p38β overcomes irinotecan and SN38 resistance both in vitro and in vivo.[6] Moreover, in CRC patients, MAPK14/p38α is required for cell proliferation and survival and its inhibition leads to cell cycle arrest and autophagy-mediated cell death.[7]

Autophagy is a highly conserved process that maintains homeostasis by eliminating unnecessary proteins or injured organelles and is responsible for the survival response to growth limiting conditions, in which cellular components are sequestered, degraded and released for recycling. It is regulated by the family of autophagy-related (*ATG*) genes. The function of autophagy in cancer is still controversial as it has been involved in mechanisms inducing either cell death or stimulating cell survival. Indeed, autophagy has been described as a tumor suppressor mechanism, because, in mice, the loss of one allele of *Becn1*, which is required for autophagy, is sufficient to promote tumorigenesis[8] and human breast epithelial carcinoma cell lines and tissue display lower level of BECN1 than normal breast epithelia.[9] However, after a cancer is established, autophagy may help cancer cells to survive in the presence of growth-limiting conditions, such as nutrient depletion and hypoxia, or cytotoxic drugs.

Here, we further investigated the functional role of MAPK14/p38α in the development of irinotecan resistance in HCT116 cells in which *TP53* was deleted (HCT116-TP53KO cells), because *TP53* is often mutated in CRC and p53 is a p38 target. We showed that, in HCT116-TP53KO cells, overexpression of constitutively active MAPK14/p38α reduces their sensitivity to SN38 and impairs cell proliferation. Moreover, MAPK14/p38α overexpression leads to an increase in autophagy and cell survival. Finally, MAPK14/p38α or autophagy inhibition increases the sensitivity of HCT116-TP53KO cells to SN38.

Results

MAPK14 is involved in SN38 resistance in HCT116-TP53KO cells. We already showed that p38, particularly MAPK14 and MAPK11, is involved in resistance to irinotecan and to its active metabolite SN38.[6] Since one of the p38 targets is TP53 and *TP53* is frequently mutated in colon cancer, we now investigated whether p38 was also involved in irinotecan resistance in cells depleted of *TP53*. To this aim, each of the four p38 isoforms (MAPK14, MAPK11, MAPK12 and MAPK13) was down-regulated by ShRNA (**Fig. 1A**) in HCT116 colorectal cancer cells, in which *TP53* was genetically ablated (HCT116-TP53KO cells) and the effect of their silencing on the sensitivity to SN38 was tested with the SRB assay (**Fig. 1B**). Silencing of the MAPK11, MAPK12 and MAPK13 had no impact on SN38 sensitivity in HCT116-TP53KO cells. On the contrary, SN38 cytotoxicity was more elevated in cells in which MAPK14 was silenced by two different hairpins (shMAPK14 and ShMAPK14bis) (**Fig. 1B**) than in control cells (shLuc), as indicated by their significantly lower IC_{50} (50% inhibitory concentration) (ShLuc 1.9 nM, shMAPK14 1.2 p = 0.03 and ShMAPKbis 1.1 p = 0.0014). This result suggests that MAPK14 loss is sufficient to increase the sensitivity of HCT116-TP53KO cells to SN38.

Then, HCT116-TP53KO cells were infected with retroviruses expressing constitutively active (CA) variant of each p38 isoform[10] and their sensitivity to SN38 was again tested using the SRB assay. Expression of the CA p38 variants was monitored by western blotting with an anti-HA antibody (**Fig. 1C**) and activity by kinase assay (**Fig. 1D**). Cells expressing constitutively active MAPK14 (HCT116-TP53KO-MAPK14CA cells) were more resistant to SN38 than control cells that were transduced with empty vector (EV) (HCT116-TP53KO-EV cells), as evidenced by their higher IC_{50} (2.6 nM and 1.3 nM, respectively, p = 0.015) (**Fig. 1E**). No difference in the IC_{50} of HCT116-TP53KO-MAPK11CA, -MAPK12CA and -MAPK13CA cell lines was observed (**Fig. 1E**).

Then, we investigated whether SN38 induces p38 phosphorylation in HCT116-TP53KO. Western blot analysis using phospho-specific p38 antibody showed an increase of p38 phosphorylation following SN38 treatment in HCT116-TP53KO (**Fig. 1F**). Overall these results show that MAPK14 is responsible for SN38 resistance and are in accordance with our previous results obtained in the parental HCT116 cell line.[6]

Expression of constitutively active MAPK14 inhibits proliferation of HCT116-TP53KO cells. To further delineate the effects of the expression of constitutively active MAPK14 in HCT116-TP53KO cells, we first compared the cell growth rates of HCT116-TP53KO-MAPK14-CA and HCT116-TP53KO-EV cells (**Fig. 2A**). Growth rates were assessed for both cell lines 14 d after retroviral transduction. In HCT116-TP53KO-MAPK14-CA cells, cell growth was greatly reduced, with a doubling time of 89.8 h compared with HCT116-TP53KO-EV, 33.3 h ($p = 9.9\ 10^{-6}$) (**Fig. 2A and B**). Since MAPK-CA overexpression did not influence cell proliferation in parental HCT116 cells (**Fig. S1A**), its negative effect on the growth rate of HCT116-TP53KO cells might be linked to the absence of *TP53*.

As these results were obtained by counting the cells at different intervals, they could be due to increased cell death or inhibition of cell proliferation. We thus compared the number of living cells and the level of apoptosis in HCT116-TP53KO-MAPK14-CA and control HCT116-TP53KO-EV cells. The percentage of annexin V-positive and 7AAD-negative cells (cells in early apoptosis) was roughly comparable in HCT116-TP53KO-EV and HCT116-TP53KO-MAPK14-CA cells (**Fig. 2D**) and also between HCT116-MAPK14-CA and HCT116-EV cells (**Fig. S1B**). In order to determine whether other cell death mechanisms could be involved, the percentage of living cells relative to the total number of cells was quantified by using the

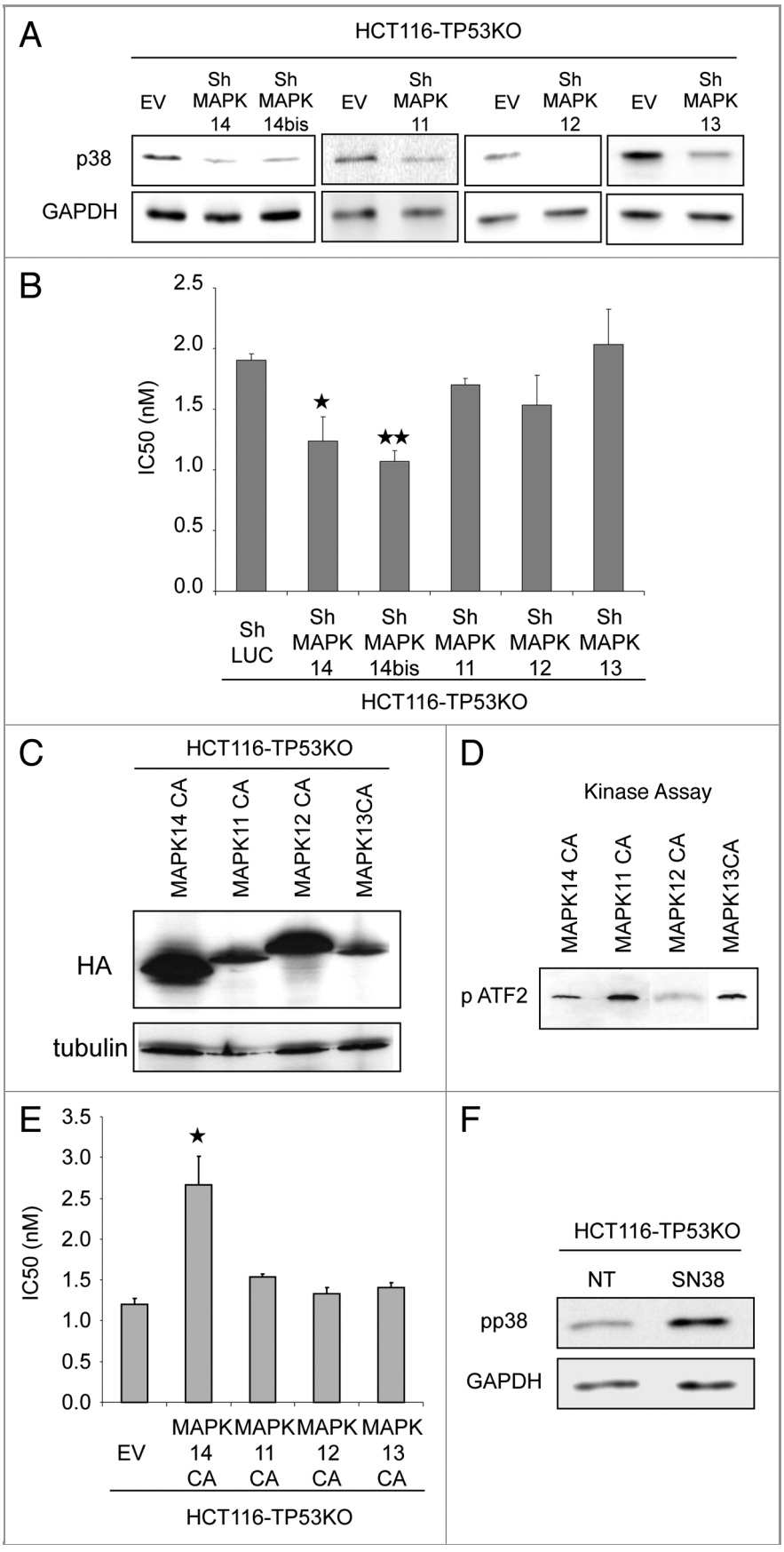

Figure 1. MAPK14 plays a role in the sensitivity to SN38 of HCT116-TP53KO cells. (A) Western blot analysis of MAPK14, MAPK14bis, MAPK11, MAPK12, MAPK13 expression in HCT116-TP53KO cells transduced with ShRNAs directed against MAPK14, MAPK11, MAPK12, MAPK13 or against *Luciferase* (ShLuc) (control). Equal loading is shown by GAPDH. (B) SRB assays to assess SN38 cytotoxicity in HCT116-TP53KO cells that stably express ShRNA targeting MAPK14, MAPK11, MAPK12, MAPK13 or *ShLuc* (control). (C) Western blot analysis (anti-HA antibody) of HCT116-TP53KO cells that express constitutively active MAPK14, MAPK11, MAPK12, MAPK13 (MAPK14-CA, MAPK11-CA, MAPK12-CA, MAPK13-CA) or empty vector (EV), as a control. Equal loading is shown by tubulin. (D) Kinase assay performed with 2 μg of recombinant MAPK14, MAPK11, MAPK12 and MAPK13 to test p38 constitutively active isoforms activity. Western blot analysis of phosphorylated ATF2. (E) SRB assay to evaluate SN38 cytotoxicity in HCT116-TP53KO cells that stably express MAPK14, MAPK11, MAPK12, MAPK13-CA or EV. (F) Western blot analysis (anti-phospho p38 antibody) of HCT116-TP53KO treated or not with SN38, 1 μM 24h00. Equal loading is shown by GAPDH.

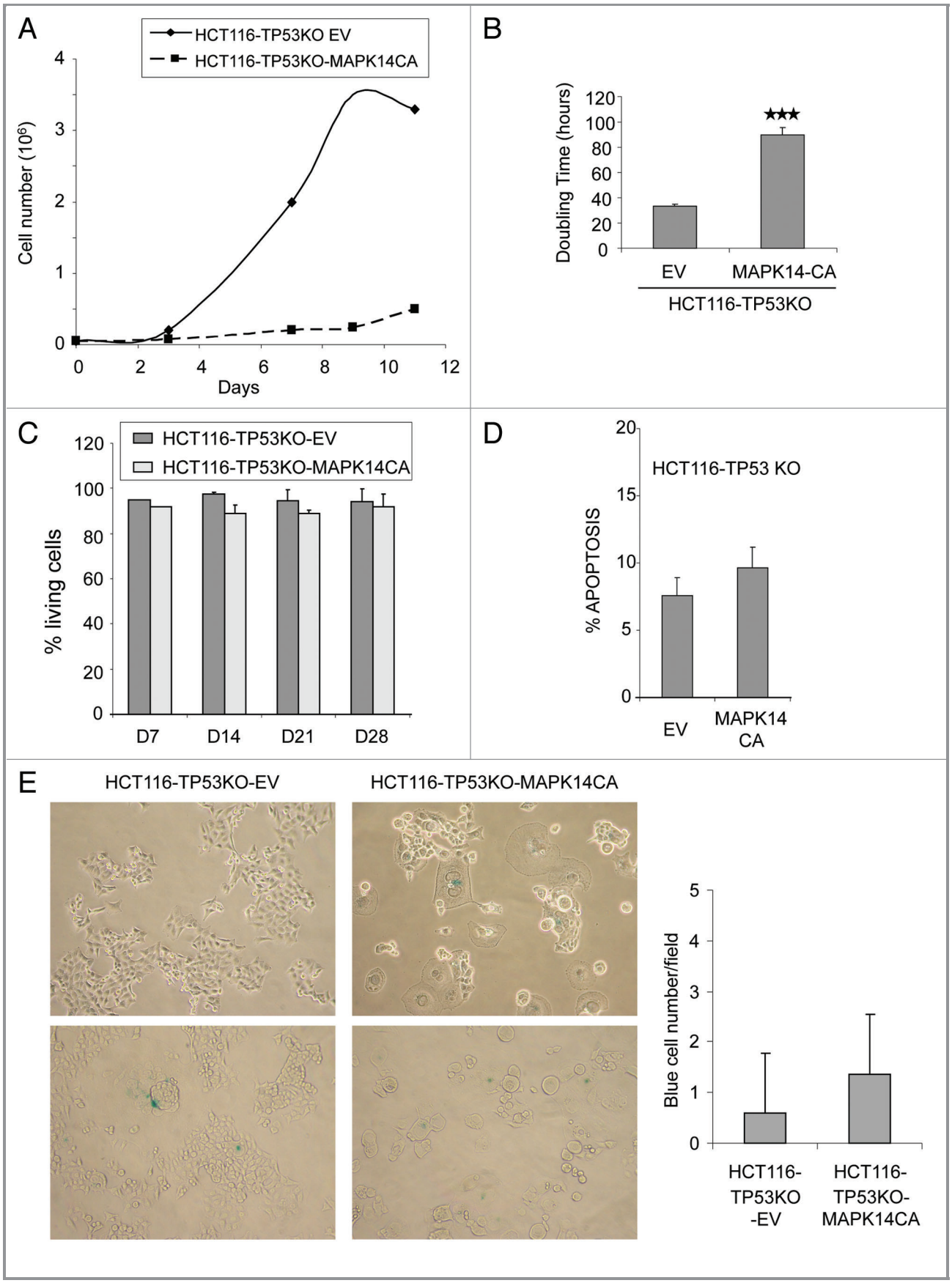

Figure 2 (See previous page). Overexpression of constitutively active MAPK14 inhibits cell growth in HCT116-TP53KO cells. (A) Growth curve of HCT116-TP53KO-EV and HCT116-TP53KO-MAPK-CA cells cultured in complete medium (10% FCS). (B) Doubling time histograms of HCT116-TP53KO-EV and HCT116-TP53KO-MAPK14-CA determined at day 14 after retroviral transduction of MAPK14-CA or EV. (C) Percentage of living cells in HCT116-TP53KO-EV and HCT116-TP53KO-MAPK14-CA cells at day (d) 7, 14, 21 and 28 after retroviral transduction. The number of viable cells was determined by counting the number of cells not stained by the Trypan blue dye. Data are representative of three independent experiments. (D) Quantification of apoptosis in HCT116-TP53KO-EV and HCT116-TP53KO-MAPK14-CA cells at day 14 after retroviral transduction of MAPK14-CA or pMSCV empty vector (EV). Apoptosis was determined by quantifying the number of 7AAD-negative and Annexin V-FLUOS-positive cells with a FACScan flow cytometer. (E) Senescence-associated β-galactosidase staining in HCT116-TP53KO-EV and HCT116-TP53KO-MAPK14-CA cells at day 14 after retroviral transduction of MAPK14-CA or EV. The number of β-galactosidase-positive (blue) cells was counted in 20 fields for each cell type.

Trypan blue exclusion method in each cell line at day 7, 14, 21 and 28 after transduction (**Fig. 2C**). No differences in the percentage of living cells were observed between control HCT116-TP53KO-EV and HCT116-TP53KO-MAPK14-CA cells at any timepoint, indicating that MAPK14 overexpression in HCT116-TP53KO cells does not increase cell death. Similar results were obtained also in HCT116-MAPK14-CA cells (**Fig. S1C**). These results indicate that HCT116-TP53KO-MAPK14-CA cells were not dying, but rather slow down their proliferation. As p38 can induce cell senescence, we then investigated whether HCT116-TP53KO-MAPK14-CA cells were senescent.[11,12] The number of cells that were positive for β-galactosidase activity (a marker of cell senescence) was similar in control and HCT116-TP53KO-MAPK14-CA cells (**Fig. 2E**), indicating that senescence is not the mechanism by which HCT116-TP53KO-MAPK14-CA cells proliferate slowly.

CDKN1A/p21 is responsible for the proliferation decrease of HCT116-TP53KO-MAPK14-CA. We then examined the cell cycle distribution of control HCT116-TP53KO-EV and HCT116-TP53KO-MAPK14-CA cells using BrdU staining and flow cytometry at day 14 after transduction (the time we observed the cell growth inhibition) (**Fig. 3A**). We observed that more HCT116-TP53KO-EV cells were in S phase (49.4%) after 15 min of BrdU labeling, in comparison with HCT116-TP53KO-MAPK14-CA cells (37.1%), indicating that the HCT116-TP53KO-MAPK14-CA cells grew more slowly. We then incubated the cells for 2, 8 and 24 h with BrdU (**Fig. 3B**) and observed that for each timepoint, BrdU incorporation was lower in HCT116-TP53KO-MAPK14-CA, confirming again the lower proliferating rate of MAPK14-CA overexpressing cells.

As the cyclin-dependent kinase (CDK) inhibitor CDKN1A/p21$^{WAF1/Cip1}$ is involved in the regulation of cell cycle inhibition[13] and is a MAPK14 target,[14] we then quantified the RNA and protein levels of CDKN1A in HCT116-TP53KO-MAPK14-CA and -EV cells at different time points after retroviral infection. CDKN1A protein expression level was increased at day 14 and 21 after retroviral infection only in HCT116-TP53KO-MAPK14-CA cells (**Fig. 3C**). Conversely, *CDKN1A* mRNA level remained unchanged in both cell lines (**Fig. 3D**). This suggests that, in HCT116-TP53KO-MAPK14-CA cells, CDKN1A overexpression is mainly due to post-translational modifications.

We then investigated whether the elevated levels of CDKN1A were responsible for the cell cycle slowdown of HCT116-TP53KO-MAPK14-CA cells. To this aim, CDKN1A expression in HCT116-TP53KO-MAPK14-CA cells was downregulated with shRNAs targeting *CDKN1A* (**Fig. 3E**) and the cell cycle distribution of such cells was again monitored using BrdU staining and flow cytometry (**Fig. 3F**). We observed that HCT116-TP53KO-Shp21-MAPK14-CA grew faster than HCT116-TP53KO-ShLuc-MAPK14-CA as indicated by a higher proportion of BrdU labeled cell (46.1% compared with 25.8%). We next incubated the cells for 4, 8 and 24 h with BrdU and confirmed that for each timepoint, that BrdU incorporation was higher in HCT116-TP53KO-Shp21-MAPK14-CA than in the control HCT116-TP53KO-ShLuc-MAPK14-CA cells (**Fig. 3G**). This result demonstrated that the reduction of cell growth was due, at least in part, to the overexpression of CDKN1A in HCT116-TP53KO-MAPK14-CA. In conclusion, MAPK14 overexpression in HCT116-TP53KO cells leads to CDKN1A overexpression and slowing down of cell proliferation.

Expression of constitutively active MAPK14 induces autophagy in HCT116-TP53KO-MAPK14-CA cells. While examining the morphology of HCT116-TP53KO-MAPK14-CA cells at day 14 after retroviral infection, we observed that they displayed large cytoplasmic vacuoles (**Fig. 4A**). This feature together with the observation that HCT116-TP53KO-MAPK14-CA cells grow slowly, but were neither apoptotic nor senescent, prompted us to investigate whether they exhibited autophagy characteristics. First, the expression of the two forms of the microtubule-associated protein 1 light chain 3 protein (LC3) was assessed by immunoblotting. Indeed, during autophagy, cytosolic LC3-I is converted into the membrane-bound lipidated LC3-II, which is detected by a mobility shift during electrophoresis. Higher LC3-II expression was observed only in HCT116-TP53KO-MAPK14-CA cells at day 14 after transduction (**Fig. 4B**, top panel), suggesting that expression of constitutively active MAPK14 in HCT116-TP53KO cells induced autophagy. A slight increase of LC3-II level was also observed in HCT116-MAPK14-CA (**Fig. S1D**). We also observed a high level of LC3-II from day 7 to day 21 after retroviral transduction of the MAPK14-CA plasmid in *TP53*-deficient H1299 lung cancer cells (**Fig. 4B**, low panel). Then, to confirm the induction of autophagy in HCT116-TP53KO-MAPK14-CA cells, cells were analyzed by electron microscopy (**Fig. 4C**). More double-membrane vacuoles, typical of early autophagic structures (arrow), were observed in HCT116-TP53KO-MAPK14-CA than in control HCT116-TP53KO-EV cells (4.4 vacuoles/cells and 1.01 vacuoles/cells, respectively; $p = 2.05\ 10^{-5}$). Similarly, transient transfection with GFP-tagged LC3 of HCT116-TP53KO-MAPK14-CA and HCT116-TP53KO-EV control cells at day 14 after retroviral transduction allowed showing that while in control cells the GFP fluorescence was diffused, in cells

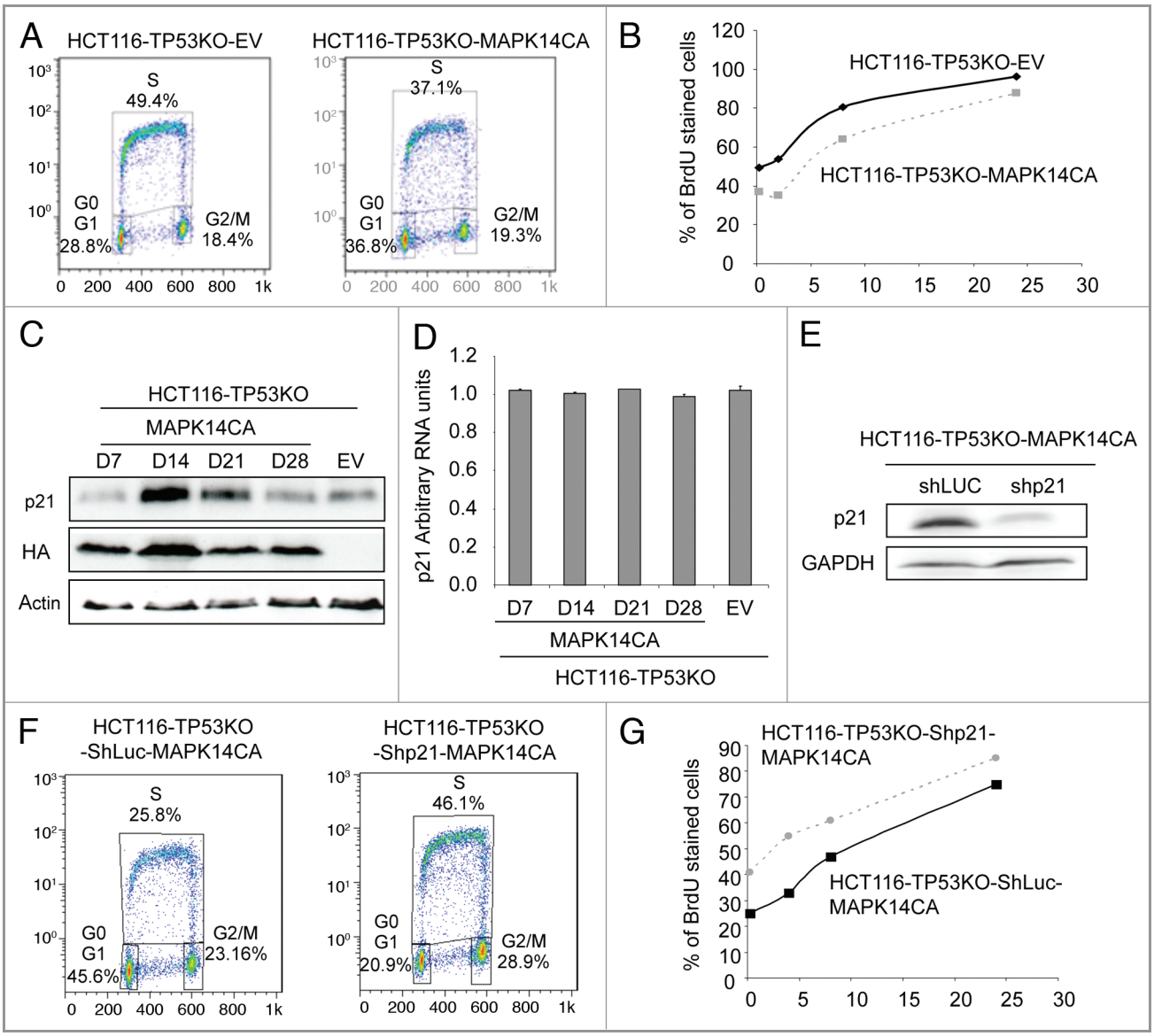

Figure 3. The proliferation inhibition of HCT116-TP53KO-MAPK14-CA cells correlates with p21 overexpression. (A) Cell cycle distribution of HCT116-TP53KO-EV and HCT116-TP53KO-MAPK14-CA cells at day 14 after retroviral transduction of MAPK14-CA or pMSCV empty vector (EV). The cell cycle distribution was evaluated after 15 min of BrDU staining with a FACScan flow cytometer. (B) Percentage of BrdU stained HCT116-TP53KO-EV and HCT116-TP53KO-MAPK14-CA cells after 15 min, 2, 8 and 24 h of BrdU incubation. (C) Western blot analysis (anti- CDKN1A antibody and anti-HA antibody to evaluate the expression of MAPK14-CA) of HCT116-TP53KO-EV (control) and HCT116-TP53KO-MAPK14-CA cells at day 7, 14, 21 and 28 following retroviral transduction (only day 14 is shown for control cells as CDKN1A level did not change). Equal loading was assessed with an anti-actin antibody. (D) *CDKN1A* mRNA levels were determined by real-time qPCR in HCT116-TP53KO-MAPK14-CA cells at days 7, 14, 21 and 28 after retroviral transduction (only day 14 for HCT116-TP53KO-EV cells as expression was unchanged). (E) Western blot analysis of CDKN1A expression in HCT116-TP53KO-MAPK14-CA and HCT116-TP53KO-EV (control) cells after retroviral transduction of ShRNA targeting *CDKN1A* (Shp21) or *Luciferase* (ShLuc), respectively. Equal loading is shown by GAPDH expression. (F) Cell cycle distribution of HCT116-TP53KO-ShLuc-MAPK14-CA and HCT116-TP53KO-Shp21-MAPK14-CA cells at day 14 after retroviral transduction. The cell cycle distribution was evaluated after 15 min of BrDU staining with a FACScan flow cytometer. (G) Percentage of BrdU stained HCT116-TP53KO-ShLuc-MAPK14-CA and HCT116-TP53KO-Shp21-MAPK14-CA cells after 15 min, 4, 8 and 24 h of BrdU incubation.

overexpressing MAPK14-CA LC3 expression was more frequently punctated (8.5 dots/cell and 2.01 dots/cell for control cells; $p = 2\ 10^{-7}$) (**Fig. 4D**).

To evaluate the relationship between reduction of growth rate and autophagy induction, we have performed LC3 western blot analysis on HCT116-TP53KO-ShLuc-MAPK14-CA and HCT116-TP53KO-Shp21-MAPK14-CA (**Fig. 4E**). We could observe that the LC3-II expression is not reduced in HCT116-TP53KO-Shp21-MAPK14-CA, while the proliferation is increased (**Fig. 3F and G**), indicating that the proliferation and the autophagy induction may not be connected. These results demonstrate that overexpression of constitutively active MAPK14

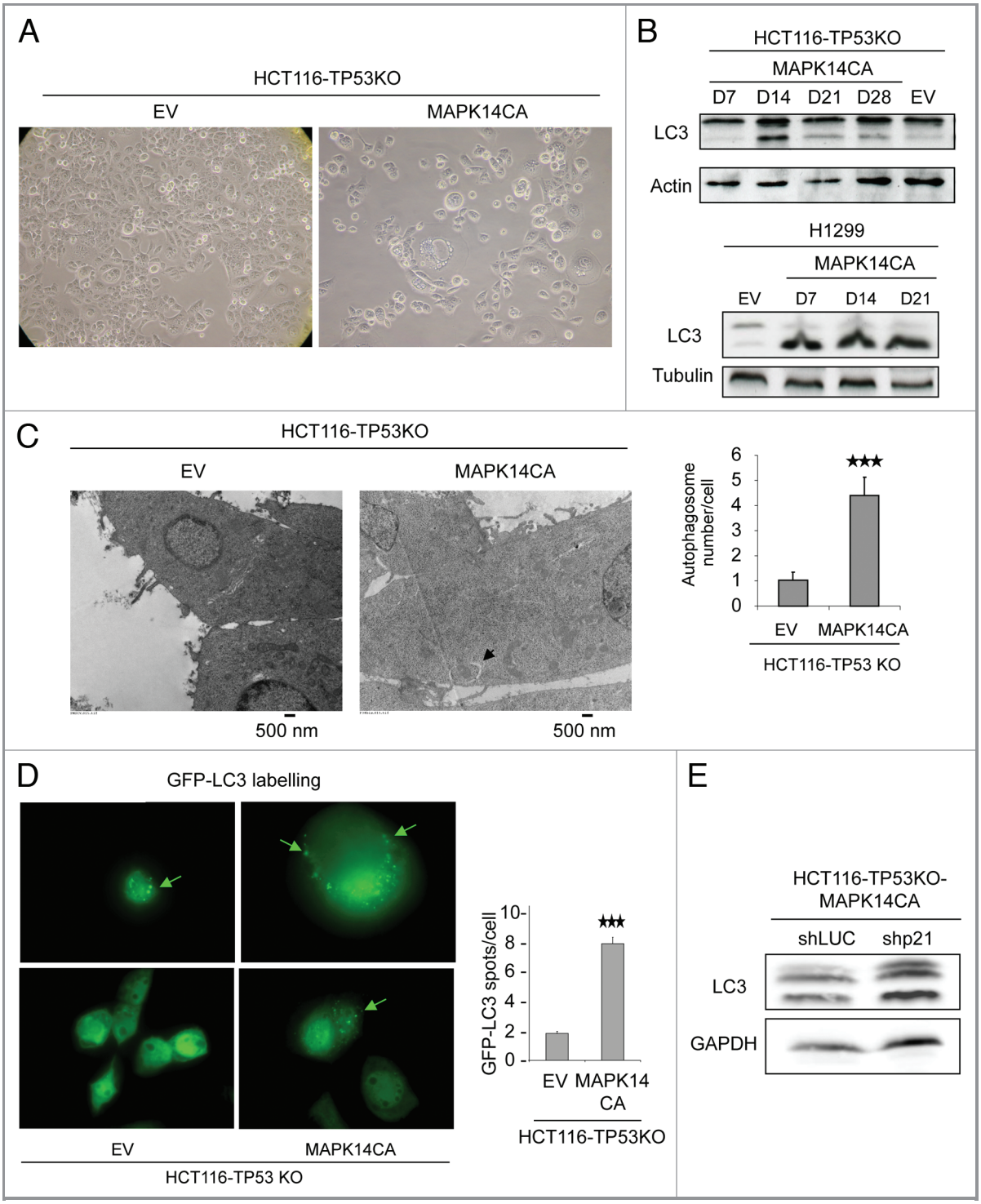

Figure 4. Overexpression of constitutively active MAPK14 induces autophagy in HCT116-TP53KO cells. (A) Phase-contrast images describing the morphology of HCT116-TP53KO-EV and HCT116-TP53KO-MAPK14-CA cells at day 14 after retroviral transduction. (B) Analysis of the expression of LC3-I and LC3-II by western blotting in HCT116-TP53KO (top panel) and H1299 (*TP53*-deficient lung cancer cells) (low panel) cells that express constitutively active MAPK14 (MAPK14-CA) or empty vector (EV), as a control at day 7, 14, 21 and 28 following retroviral transduction. Only day 14 is shown for cells transduced with EV as LC3 expression was unchanged. Equal loading is shown by actin expression. (C, left panel) Electron micrographs of HCT116-TP53KO-EV and HCT116-TP53KO-MAPK14-CA cells at day 15 after retroviral transduction. Arrow indicates the presence of a double-membrane vacuole. (C, right panel) Number of autophagosomes/cell in HCT116-TP53KO-EV and HCT116-TP53KO-MAPK14-CA cells at day 15 after retroviral transduction (100 cells were counted for each cell type). (D, left panel) HCT116-TP53KO-EV and HCT116-TP53KO-MAPK14-CA cells expressing GFP-LC3 were analyzed by immunofluorescence. The pattern of GFP-LC3 expression in the cytosol changed from diffuse to punctate/vesicular. (D, right panel) The number of vesicular GFP-LC3 spots/cell in HCT116-TP53KO-EV and HCT116-TP53KO-MAPK14-CA cells was scored (100 cells were counted for each cell type). The results are represented as the mean ± SD. (E) Western blot analysis (anti-LC3 antibody) of HCT116-TP53KO-ShLuc-MAPK14-CA and HCT116-TP53KO-Shp21-MAPK14-CA cells. Equal loading is shown by GAPDH.

inhibits cell proliferation and induces autophagy in *TP53*-depleted colon cancer cells. As a consequence, decreases in cell proliferation and autophagy induction can both be involved in MAPK14 induced resistance to SN38.

MAPK14-induced autophagy promotes survival of HCT116-TP53 KO-MAPK14-CA cells. Autophagy is a dynamic process that begins with the generation of autophagosomes and terminates with their degradation in lysosomes and corresponds to the autophagic flux. To examine the autophagic flux in HCT116-TP53KO-MAPK14-CA cells, we monitored the expression of SQSTM1/p62, which is incorporated into the completed autophagosome and degraded in autolysosomes.[15] Western blot analysis of SQSTM1 expression (**Fig. 5A**) indicates that, in HCT116-TP53KO-MAPK14-CA cells, SQSTM1 is degraded from day 14 to day 28 after MAPK14-CA transduction. To confirm this result, we have also compared the half-life of SQSTM1 in HCT116-TP53KO-MAPK14-CA and in HCT116-TP53KO-EV after shutting off protein synthesis with cycloheximide (**Fig. 5B**) at day 14 after retroviral transduction. Cycloheximide-chase experiment indicated that SQSTM1 is unstable in HCT116-TP53KO-MAPK14-CA but not in HCT116-TP53KO-EV cells. These results indicate that MAPK14-CA expression induces functional autophagic flux. Incubation with 3-methyladenine (3MA), an inhibitor of class III phosphatidylinositol 3-kinase (PtdIns3K), which blocks the early steps of autophagy,[15] decreased LC3-II expression in HCT116-TP53KO-MAPK14-CA and in HCT116-TP53KO-EV control cells in comparison to untreated cells (NT) (**Fig. 5C**). Finally, incubation with bafilomycin A_1 (Baf), which alters the lysosomal pH and inhibits lysosomal degradation,[15] increased the expression level of LC3-II in both HCT116-TP53KO-EV and HCT116-TP53KO-MAPK14-CA cells in comparison to untreated cells (NT), indicating a stabilization of LC3-II probably due to an increase in the number of autophagosomes as a result of the inhibition of lysosomal degradation. The lower LC3-II expression after 3MA treatment and the higher LC3-II expression after treatment with Baf demonstrate a complete execution of the autophagic pathway, reinforcing our hypothesis that MAPK14 induce functional autophagy.

We next evaluated the impact of MAPK14−induced autophagy on cell survival. To this end, we inhibited autophagy either pharmacologically or genetically and evaluated cell viability using the Trypan blue exclusion method. First, HCT116-TP53KO-EV and HCT116-TP53KO-MAPK14-CA cells were incubated with Baf or 3MA (**Fig. 5D**). Both autophagy inhibitors did not have any effect on the cell viability of control HCT116-TP53KO-EV cells, whereas in HCT116-TP53KO-MAPK14-CA cells they significantly reduced the number of viable cells in comparison to untreated cells (NT) (3MA: 31% of dead cells, $p = 0.00014$; bafilomycin: 47.5%, $p = 0.00003$). These results were confirmed by downregulating the expression of *ATG5* and *ATG7*, two genes which are essential for autophagy, with specific siRNAs (**Fig. 5E**). Indeed, downregulation of *ATG5* or *ATG7* strikingly increased cell mortality in HCT116-TP53KO-MAPK14-CA cells (but not in in HCT116-TP53KO-EV cells) in comparison to cells transfected with control siRNAs (siCT) (siATG5: 88% of dead cells, $p = 1\ 10^{-8}$; siATG7: 90%, $p = 1.9\ 10^{-7}$). In conclusion, these data demonstrate that overexpression of constitutively active MAPK14 induces survival-promoting autophagy in HCT116-TP53KO cells.

Autophagy is involved in SN38 resistance of TP53-defective cancer cells. As MAPK14 overexpression in HCT116-TP53KO cells induces survival autophagy, we then investigated whether autophagy could play a role in the mechanism of cancer cell resistance to SN38. We first assessed autophagy induction with SN38 by LC3 labeling immunofluorescence in HCT116 (**Fig. S2A**) and HCT116-TP53KO (**Fig. 6A**). The untreated cells (NT) presented a diffuse LC3 staining while SN38 treated cells presented punctated labeling (**Fig. 6A**). We then treated HCT116, HCT116-TP53KO and the *TP53* mutated colorectal cancer cells, SW480, with 1 μM SN38 for 24 h (**Fig. 6B**; **Fig. S2B**) and performed LC3 western blot analysis. The LC3-II expression was increased in SN38 treated cells in comparison to untreated cells (NT), indicating that SN38 can induce autophagy in HCT116, HCT116-TP53KO and SW480 cells. To address the autophagic flux, we have co-treated HCT116-TP53KO cells with Baf and SN38, and observed that these cells display more LC3-II labeling than HCT116-TP53KO treated with SN38

Figure 5 (See next page). Autophagy in HCT116-TP53KO-MAPK14-CA cells promotes cell survival. (A, top panel) Western blot analysis of SQSTM1/p62 expression in HCT116-TP53KO-MAPK14-CA cells at day 7, 14, 21 and 28 following retroviral transduction (only day 14 is shown for control HCT116-TP53KO-EV cells as expression did not change). Equal loading is shown by actin expression. (A, bottom panel) Quantification of SQSTM1 expression relative to β-actin in control HCT116-TP53KO-EV (day 14) and HCT116-TP53KO-MAPK14-CA cells at day 7, 14, 21 and 28 following retroviral transduction. (B, top panel) Western blot analysis of SQSTM1 expression in HCT116-TP53KO-EV and HCT116-TP53KO-MAPK14-CA cells at day 14 following retroviral transduction after cycloheximide chase (2, 4 and 8 h of cycloheximide treatment). Equal loading is shown by GAPDH expression. (B, bottom panel) Quantification of SQSTM1 expression relative to GAPDH in HCT116-TP53KO-EV and HCT116-TP53KO-MAPK14-CA cells at day 14 following retroviral transduction after cycloheximide chase. (C, left panel) Western blot analysis of the expression of LC3-I and LC3-II in HCT116-TP53KO-MAPK14-CA and control HCT116-TP53KO-EV cells at day 14 after retroviral transduction following incubation or not (NT) with 3-methyladenine (3MA) or bafilomycin A_1 (Baf). Equal loading is shown by actin expression. (C, right panel) Quantification of LC3-II expression relative to β-actin in control and HCT116-TP53KO-MAPK14-CA cells incubated or not (NT) with 3MA or Baf. (D) Cell viability of HCT116-TP53KO-MAPK14-CA and control HCT116-TP53KO-EV cells at day 14 after retroviral transduction, incubated or not with 3-methyladenine (3MA) or bafilomycin A_1 (Baf) for 72 h. The number of viable cells was determined by counting the cells not stained with the Trypan blue dye. Data are representative of three independent experiments. (E, top panel) Cell viability of HCT116-TP53KO-MAPK14-CA and control HCT116-TP53KO-EV cells at day 14 after retroviral transduction, following transfection with control siRNA or anti-*ATG5* or -*ATG7* siRNAs. The number of viable cells was determined by counting the cells not stained with the Trypan blue dye. Data are representative of three independent experiments. (E, bottom panel) Western blot analysis of ATG5 and ATG7 expression in HCT116-TP53KO-MAPK14-CA cells at day 2 (d2) and 4 (d4) after transfection with control siRNA or anti-*ATG5* or -*ATG7* siRNAs (similar results were obtained for HCT116-TP53KO-EV). Equal loading is shown by actin expression.

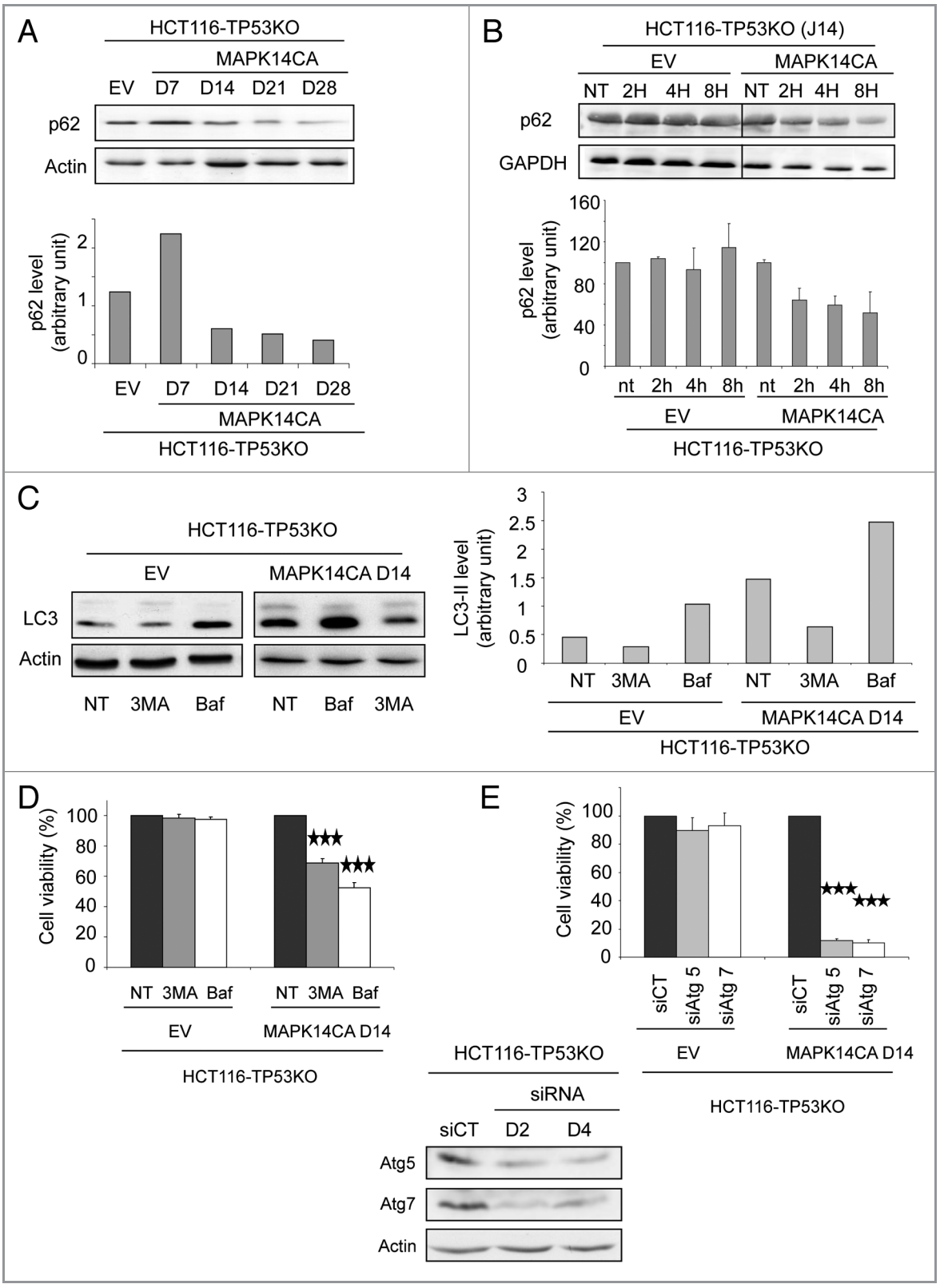

Figure 5. For figure legend, see page 1105.

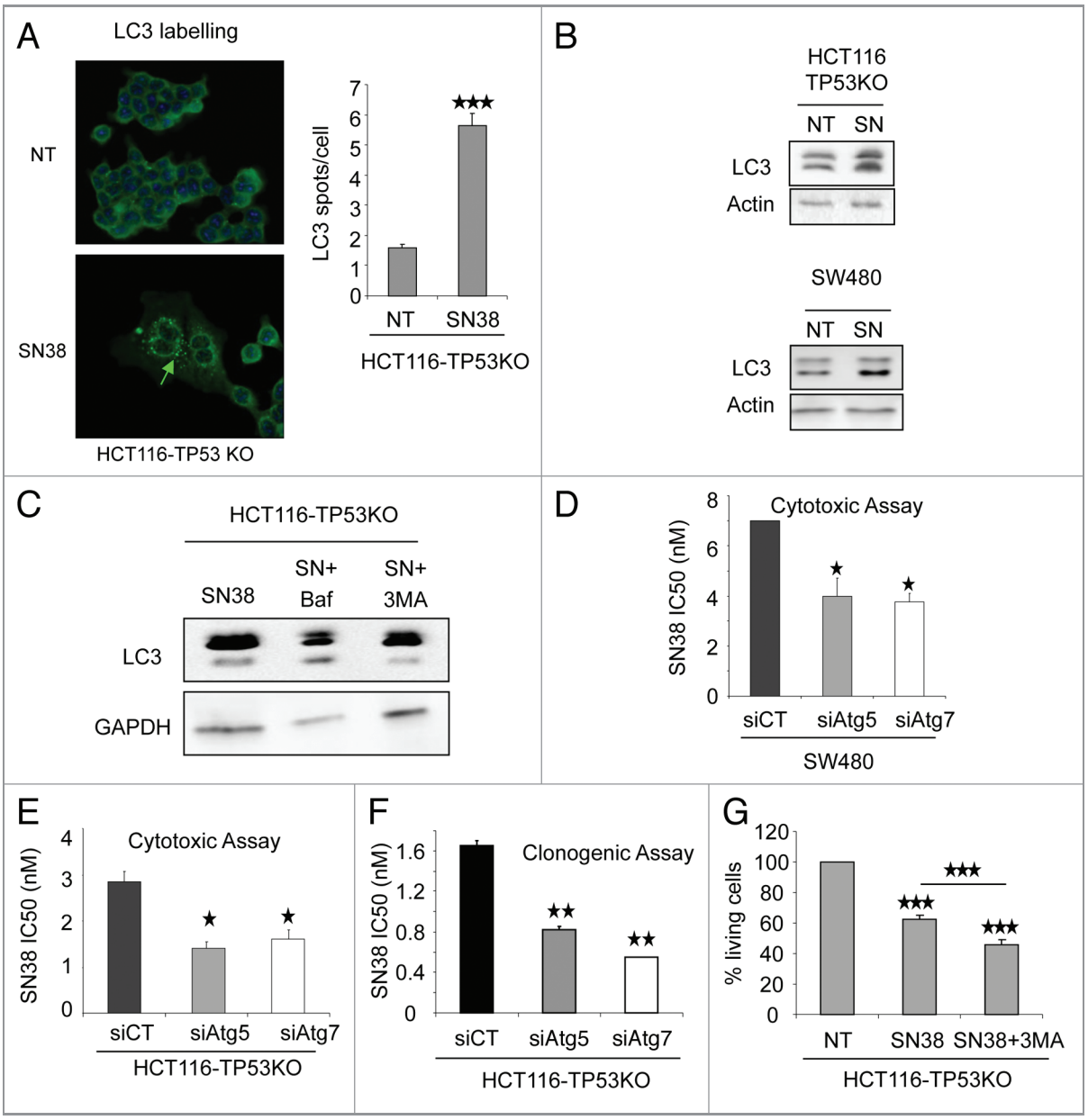

Figure 6. Inhibition of autophagy enhances the cytotoxic effect of SN38 on p53-defective colorectal cancer cells. (A, left panel) LC3 staining analyzed by immunofluorescence of HCT116-TP53KO cells treated or not (NT) with 1 μM SN38 for 24 h. The pattern of LC3 expression in the cytosol changed from diffuse to punctate/vesicular. (A, right panel) The number of vesicular LC3 spots/cell in HCT116-TP53KO cells treated or not with 1 μM SN38 for 24 h was scored (100 cells were counted for each cell type). The results are represented as the mean ± SD. (B) Western blot analysis of LC3-I and LC3-II expression in HCT116-TP53KO and SW480 cells treated or not (NT) with 1 μM SN38 for 24 h. Equal loading is shown by actin expression. (C) Western blot analysis of HCT116-TP53KO treated with Baf, SN38, SN38+Baf and SN38, SN38+3MA. Equal loading is shown by GAPDH expression. (D) SRB assays to assess SN38 cytotoxicity in SW480 cells transfected with control siRNA or anti-*ATG5* or -*ATG7* siRNAs. (E) SRB assays to assess SN38 cytotoxicity in HCT116-TP53KO cells transfected with control siRNA or anti-*ATG5* or -*ATG7* siRNAs. (F) Clonogenic assay to assess SN38 cytotoxicity in HCT116-TP53KO cells transfected with control siRNA or anti-*ATG5* or -*ATG7* siRNAs. (G) Percentage of living cells in HCT116-TP53KO treated with SN38 or SN38 + 3MA. The number of viable cells was determined by counting the number of cells not stained by the Trypan blue dye. Data are representative of three independent experiments.

alone (**Fig. 6C**). Conversely, HCT116-TP53KO cells incubated with 3MA+SN38 presented a lower LC3-II level compared with cells treated with SN38 alone. Both results indicate that SN38 induced functional autophagy in HCT116-TP53KO.

We then inhibited autophagy in HCT116, HCT116-TP53KO and SW480 cells and tested the effect of such inhibition on the sensitivity to SN38. SW480 cells were transfected with *ATG5*- or *ATG7*-specific siRNAs and SN38 cytotoxicity, assessed by SRB assay, was evaluated. We found that SN38 IC_{50} was lower in cells in which autophagy was inhibited (**Fig. 6D**) than in cells transfected with control siRNAs (siCT), indicating that autophagy is involved in SN38 resistance. We confirmed the impact of

autophagy inhibition on SN38 cytotoxicity in HCT116 TP53KO cells with siATG transfection and 3MA treatment, using SRB (**Fig. 6E**), clonogenic (**Fig. 6F**) and Trypan blue exclusion assay (**Fig. 6G**), confirming the protective role of autophagy on SN38 treatment. At the opposite, autophagy inhibition with siATG transfection or 3MA treatment was not able to impact on SN38 cytotoxicity in HCT116 cells (**Fig. S2D–S2F**), indicating that SN38 induces autophagy-mediated survival only in *TP53*-defective cells. In conclusion, similarly to what we observed following inhibition of MAPK14,[6] inhibition of autophagy enhanced the cytotoxic effect of SN38, but only in cells where TP53 is altered.

As we have previously observed that the two other drugs used to treat colorectal cancer, 5-fluorouracil (5-FU) and oxaliplatin, induced p38 phosphorylation, we asked whether these drugs can induce autophagy, and if autophagy has an impact on their cytotoxicity (**Fig. S3**). We first determined IC_{50} concentrations for both drugs using SRB assay (**Fig. S3A**), and found 0.4 µM for HCT116, 1.4 µM for HCT116-TP53KO concerning oxaliplatin and 4 µM for 5-FU for both cell lines. We then treated the cells with 5-FU and oxaliplatin at the IC_{50} concentration during 96 h and determine the autophagy level. Western blot monitoring LC3 showed that neither 5-FU nor oxaliplatin induced autophagy (**Fig. S3B**). We then inhibited autophagy by transfecting HCT116 and HCT116-TP53KO with *ATG5*- or *ATG7*-specific siRNAs and tested the effect of such inhibition on the sensitivity to 5-FU and oxaliplatin using the SRB assay. We observed that autophagy inhibition did not impact the 5-FU and oxaliplatin cytotoxicity in HCT116 and HCT116-TP53KO cells (**Fig. S3C–S3F**).

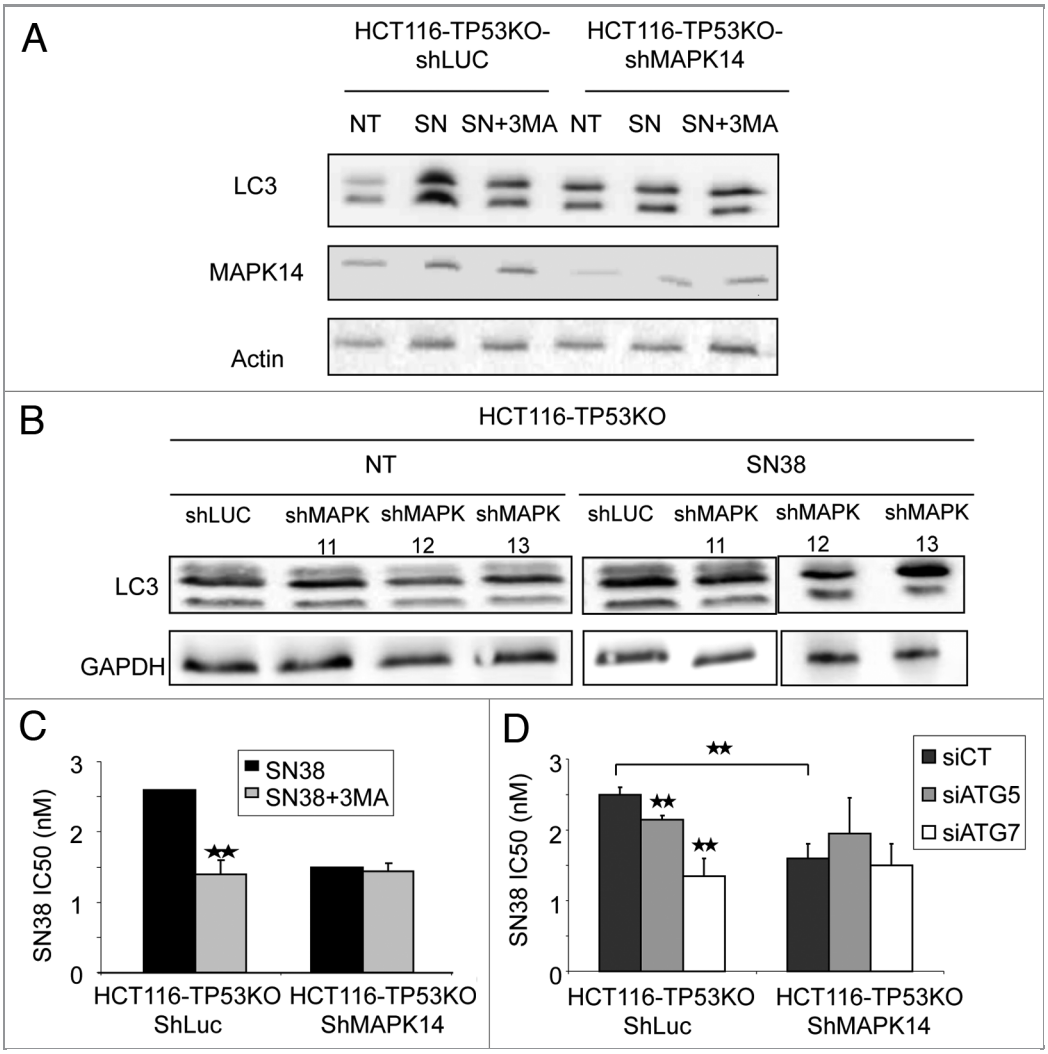

Figure 7. Involvement of autophagy in SN38 resistance depends upon MAPK14. (A) Western blot analysis of LC3-I and II and MAPK14 expression in HCT116-TP53KO-ShLuc and HCT116-TP53KO-ShMAPK14 cells after treatment or not (NT) with 2 nM SN38 alone (SN) or with 10 nM 3-methyladenine (SN+3MA) for 96 h. (B) Western blot analysis of LC3-I and II of HCT116-TP53KO-ShLuc, HCT116-TP53KO-ShMAPK11, HCT116-TP53KO-ShMAPK12 and HCT116-TP53KO-ShMAPK13 cells after treatment or not (NT) with 2 nM SN38 alone (SN) for 96 h. (C) SRB assays to assess the cytotoxicity of SN38 alone or in combination with 3-methyladenine (SN38+3MA) in HCT116-TP53KO-ShLuc and HCT116-TP53KO-ShMAPK14 cells. (D) SRB assays to assess SN38 cytotoxicity of HCT116-TP53KO-ShLuc and HCT116-TP53KO-ShMAPK14 cells transfected with control siRNA or anti-*ATG5* or -*ATG7* siRNAs.

We finally asked whether SN38-mediated induction of autophagy is MAPK14-dependent. To answer this question, we downregulated, or not (HCT116-TP53KO-ShLuc cells), the expression of MAPK14 with a specific shRNA (ShMAPK14) in HCT116-TP53KO cells and incubated them with 2 nM SN38 for 96 h. Western blot analysis (**Fig. 7A**) showed that SN38 induced higher LC3-II levels in control HCT116-TP53KO-ShLuc (as expected), but not in HCT116-TP53KO-ShMAPK14. Concomitant incubation of cells with 2 nM SN38 and 10 nM 3MA, which inhibits autophagy, for 96 h prevented the LC3-II increase observed in HCT116-TP53KO-ShLuc cells treated with SN38 alone, but did not have any effect on HCT116-TP53KO-ShMAPK14 cells (**Fig. 7A**). This result clearly indicates that MAPK14 is necessary for SN38-mediated induction of autophagy. In addition to MAPK14, we have also performed inhibition of MAPK11, MAPK12 and MAPK13 and treated the HCT116-TP53KO cells with SN38. LC3-II western blot analysis indicates that inhibition of MAPK11, MAPK12 and MAPK13 did not inhibit the SN38 autophagy induction (**Fig. 7B**). Moreover, we have treated HCT116-ShLuc and HCT116-shMAPK14 cells with SN38 and we found that autophagy is not reduced in HCT116-ShMAPK14 (**Fig. S2C**). In conclusion, ShMAPK14 is the main p38 isoform involved in autophagy induction by SN38 (**Fig. 7A**), and exclusively in a *TP53*KO context.

We then evaluated the impact of autophagy inhibition on the sensitivity to SN38 of HCT116-TP53KO-ShMAPK14 cells. HCT116-TP53KO-ShLuc and HCT116-TP53KO-ShMAPK14 cells were either treated with SN38 and SN38+3MA (**Fig. 7C**) or transfected with siATG5 and siATG7 (**Fig. 7D**), and their IC_{50} were determined. Autophagy inhibition increased the SN38 cytotoxic effect in control HCT116-TP53KO-ShLuc cells, but not in HCT116-TP53KO-ShMAPK14 cells. These results suggest that MAPK14 activation and survival-promoting autophagy are part of the same mechanism induced by SN38, and that hindering MAPK14 activity will block the SN38 effect on survival-promoting autophagy. In conclusion MAPK14 confers SN38 resistance to HCT116-TP53KO cells by inducing survival autophagy.

Discussion

In this study, we demonstrated the role of MAPK14 in the resistance to SN38, the active metabolite of irinotecan, in *TP53*-depleted HCT116 colorectal cancer cells. Moreover we showed that overexpression of constitutively active MAPK14 induces survival autophagy in colorectal cancer cells depleted of *TP53* and that inhibition of autophagy in such cells enhances the cytotoxic effect of SN38.

We previously reported that MAPK14 is involved in irinotecan resistance in in vivo and in vitro experimental settings and in clinical samples.[6] Here we confirm this finding by showing that overexpression of constitutively active MAPK14 makes also *TP53*-depleted colorectal cancer cells more resistant to irinotecan, and conversely its downregulation sensitizes these cells. This new finding indicates that the involvement in irinotecan resistance is not dependent on the TP53 status of the cancer cells. This suggests that p38 inhibitors could be used as an adjuvant therapy to potentiate the efficacy of irinotecan-based chemotherapies, whatever the TP53 status of the tumor.

Moreover, we report that overexpression of MAPK14 leads to cell growth inhibition of HCT116-TP53KO cells. Previous works have already reported that MAPK14 can cause cell cycle arrest via two pathways. Specifically, after UV radiation, MAPK14 can phosphorylate and inhibit the phosphatase CDC25B, which in turn inhibits the CCNB/cyclin B-CDK1/CDC2 complex needed for cell cycle progression.[16] The other pathway involves the phosphorylation and activation of TP53 and induction of the TP53-dependent G_2/M checkpoint.[13] Here, we showed that MAPK14 overexpression leads to an increase of CDKN1A protein (but not of mRNA) level even in the absence of TP53 and that CDKN1A upregulation is responsible for proliferation inhibition. Our findings are in agreement with the work by Kim and colleagues who demonstrate that MAPK14 can phosphorylate directly CDKN1A, leading to CDKN1A stabilization.[17]

It is well known that p38 has a dual role in autophagy, both as a positive and negative regulator. Our results show that, in HCT116-TP53KO cells, MAPK14 can induce autophagy which in turn promotes cell survival. Similarly, Tang et al., reported that, in the mouse model of Alexander disease, p38 is involved in GFAP accumulation in astrocytes and in the induction of survival-promoting autophagy. Furthermore, Cui et al., described that, in HeLa cells, oridonin induces autophagy through p38 activation.[18,19] On the other hand, Comes and colleagues found that, in colon cancer cells, p38 inhibition leads to autophagy and apoptosis,[20] and Webber et al., showed that p38 negatively regulates autophagy by inhibiting the interaction of ATG9 with FAM48A/p38IP in starvation conditions.[21] Although these results seem contradictory, our hypothesis is that the role of p38 in autophagy depends on the nature of the stimulus, the strength and duration of p38 activation and the *TP53* status. Moreover, it is important to differentiate the autophagy promoting cell survival from the autophagy leading to cell death as they may involve different signaling pathways.

It has already been reported[22] that camptothecin can induce autophagy in breast cancer cells. When this autophagic response is inhibited, camptothecin-induced apopotic cell death is increased, suggesting that autophagy might play a role in a drug-resistance mechanism. Our data demonstrated that the camptothecin-derivative SN38 activates autophagy also in colon cancer cells, a more relevant cancer model since camptothecin-derivative drugs are used in the clinic to treat patients with CRC (but not for breast cancer). It was recently shown that 5-fluorouracil (5-FU), a drug widely used in combination with irinotecan in the clinic (FOLFIRI protocol), also induces autophagy in HCT116 and DLD-1 colorectal cancer cells[23] and inhibition of 5-FU-induced autophagy increases cell death. We did not reproduce these data, most probably because we treated the cells with lower concentration of autophagy inhibitor. We rather showed that inhibition of MAPK14-mediated autophagy in our model can increase the sensitivity of colon cancer cells to SN38 cytotoxic effect. It would be interesting to test the combination of

irinotecan+autophagy inhibitor and to treat nonresponder patients who receive FOLFIRI with an autophagy inhibitor.

Our findings also indicate that the *TP53* status is crucial because autophagy inhibition does not increase the cytotoxic effect of SN38 in colorectal cancer cells with wild-type *TP53*. p53 can modulate autophagy depending on its cellular localization.[24] Indeed, nuclear p53 will act as a transcription factor and transactivate several autophagy inducers (such as DRAM1, SESN2/Sestrin2, BAX and BBC3/PUMA) to induce autophagy and facilitate apoptosis. Conversely, cytoplasmic TP53 inhibits autophagy by an unknown mechanism. Here, we show that in the absence of TP53, overexpression of MAPK14 (by retroviral transduction of constitutively active MAPK14 or upon treatment with SN38) can induce survival-promoting autophagy.

Growing evidence indicates that chemotherapy induces autophagy in a variety of tumor cells,[25] leading either to tumor protection or tumor cell death. In the present study, we demonstrated that, in *TP53* defective colorectal cancer cells, camptothecin-derivative drugs induce survival-promoting autophagy via MAPK14 activation. In conclusion, it appears that survival-promoting autophagy, which is responsible for resistance to chemotherapy, is dependent on the *TP53* status of the tumor and TP38 activation. As autophagy inhibitors could be used to overcome camptothecin-related drug resistance, it is crucial to determine the *TP53* status of the patients and the level of p38 activation by the drug.

Materials and Methods

Cell lines and reagents. The HCT116 (CCL-247), SW480 (CCL228) human colon adenocarcinoma cell lines and the H1299 (CRL5803) human non-small cell lung cancer cell line from ATCC were grown in RPMI 1640 supplemented with 10% fetal calf serum (FCS) and 2 mmol/L l-glutamine at 37°C in a humidified atmosphere with 5% CO_2. HCT116-TP53KO cells, in which *TP53* had been genetically ablated, were kindly given by Bert Volgestein. SN38 was provided by Sanofi-Aventis.

Drug sensitivity. Cell growth inhibition and cell viability after SN38 treatment were assessed using the sulforhodamine B (SRB) (Sigma, S-9012) assay as previously described and called SRB assays.[6]

Western blot analyses. Western blot analysis of cell extracts from control and retrovirus-infected cells were performed as previously described.[6] Primary antibodies were directed against CDKN1A (CST-2947), MAPK14/p38α (CST-9218), tubulin (CST-2125) (Cell Signaling Technology), LC3 (Sigma Aldrich, L7543), SQSTM1/p62 (BD Transduction Laboratory, 610833), actin (Abcam, ab8227), GAPDH (Abcam, ab9482). Secondary antibodies were horseradish peroxidase-conjugated anti-mouse (sc-2314) or anti-rabbit (sc-2004) antisera (Santa Cruz).

Ultrastructural evaluation. Cells were immersed in a solution of 2.5% glutaraldehyde in 0.1 M Sorensen's buffer (NaH_2PO_4 and Na_2HPO_4, pH 7.4) at 4°C overnight. They were then rinsed in Sorensen's buffer and post-fixed in 0.5% osmic acid in the dark and at room temperature for 2 h. After two rinses in Sorensen's buffer, cells were dehydrated through a graded series of ethanol solutions (30–100%) and embedded in EmBed 812 (EMS 14120) using an Automated Microwave Tissue Processor for Electronic Microscopy (Leica EM AMW). Thin 70 nm sections were cut with a Leica-Reichert Ultracut E microtome at different levels of each block and were counterstained with uranyl acetate. Cell structures were assessed using a Hitachi 7100 transmission electron microscope at the Centre de Ressources en Imagerie Cellulaire de Montpellier (France). The number of autophagosomes was evaluated in 100 cells for each cell type.

Cell senescence. Senescent cells were identified by detecting β-galactosidase activity at pH 6, a known marker of cell senescence. Cells were plated on 12-mm glass coverslips in culture dishes. After 48 h, they were fixed in 2% paraformaldehyde/0.2% glyceraldehyde, and then incubated with the staining solution (20 mg/ml X-Gal (5-bromo-4-chloro-3-indolyl-β-D-galactopyranoside); 40 mM citric acid/sodium phosphate, pH 6.0; 5 mM potassium ferrocyanide; 150 mM NaCl; 2 mM $MgCl_2$)[26] overnight. The number of stained cells was evaluated in 20 fields (using a 63× NA objective and a Leica inverted microscope) for each cell type.

GFP-LC3 expression. Cells were plated on 12-mm glass coverslips in culture dishes and transiently transfected with the expression plasmid encoding the chimeric protein pEGFP-LC3 (a generous gift from Dr. L. Espert, Montpellier, France) using Lipofectamine (Invitrogen, 18324012) according to the manufacturer's instructions. Transfected cells were then fixed in 3.7% formaldehyde, mounted in Moviol, and images were recorded using a 63 × NA objective and a Leica inverted microscope. Autophagosomes were counted in 100 cells for each cell type.

Retroviral infection. HCT116-TP53KO cells that stably express the constitutively active (CA) p38 isoforms were obtained by retroviral transduction of the pMSCV-MAPK14-CA, pMSCV-MAPK11-CA, pMSCV-MAPK12-CA and pMSCV-MAPK13-CA plasmids. MAPK14 mutant is $p38\alpha^{D176A\ F327S}$, MAPK11 mutant is $p38\beta^{D176A}$, MAPK12 mutant is $p38\gamma^{D179A}$ and MAPK13 mutant is $p38\delta^{F324S}$. Control cells were transduced with the pMSCVhyg (Clontech, 6344001) empty vector (EV) (HCT116-TP53KO-EV cells). Twenty-four hours after transduction, cells were selected with 1 μg/mL hygromycin. HCT116-TP53KO-EV or –MAPK14-CA cells were co-infected with the pSIREN (Clontech, 631526) vector in which the short hairpin RNAs (shRNA) targeting *CDKN1A* was cloned. Cells were selected with 0.5 μg/mL puromycin and with 0.5 μg/mL hygromycin. HCT116-TP53KO cells expressing ShRNAs targeting, *MAPK14, MAPK14bis, MAPK11, MAPK12* and *MAPK13* mRNA were obtained by retroviral gene transduction of the pSIREN vector in which the ShRNAs were cloned. Two different hairpins had been used targeting different part of the MAPK14 mRNA (ShMAPK14 and ShMAPK14bis). Cells were selected with 1 μg/mL of puromycin and then stable clones were pooled. The shRNA targeting *Luciferase* (shLuc) was used as negative control.

Autophagy inhibition. Two autophagy inhibitors were used: 3-methyladenine (3MA) (M9281), a phosphatidylinositol 3-kinase inhibitor that inhibits the formation of autophagosomes, and bafilomycin A_1 (11707), a V type proton pump that inhibits the formation of secondary lysosomes (both from Sigma Aldrich).

HCT116-TP53KO-EV or –MAPK14-CA cells (0.75×10^6) were grown in 6-well plates for 48 h and then incubated with 10 nM 3-methyladenine or 50 nM bafilomycin A_1 for 48 h. Cell viability was then estimated using the Trypan blue exclusion method.

For studying the autophagic flux, 0.1×10^6 HCT116-TP53KO-EV or -MAPK14-CA cells were grown in 6-well plates for 72 h and then incubated with 10 nM 3-methyladenine or 50 nM bafilomycin A_1 for 96 h.

For SRB assays, cells were plated in 96 well plates and treated during 96 h with SN38 alone or with SN38+3MA (10 nM) or SN38 + Baf (50 nM).

The cells are treated with a very low concentration of 3-MA (10 nM) when the treatment is 48, 72 or 96 h. This 3-MA concentration avoids the nonspecific side effect, is sufficient to inhibit autophagy induction and is not toxic for control cells.

SQSTM1 degradation was evaluated by cycloheximide-chase experiments in HCT116-TP53KO-EV and HCT116-TP53KO-MAPK14-CA.

Cell growth assay. Cells (5×10^4) were seeded in 6-well plates in triplicate. Six identical plates were seeded for each counting experiment. Every 24 h after plating, cells were counted in one of the plates.

Cell cycle analysis. *BrdU labeling.* Cells were incubated continuously with 30 μM of 5-bromo-2-deoxyuridine (BrdU, B9285, Sigma) for the indicated times. Cells were harvested, centrifuged at 1200 rpm for 5 min, washed in PBS, and resuspended in 75% ethanol by vortexing before storage at 4°C for 24 h. After a pepsin treatment cells were resuspended in 2 M hydrochloric acid, washed and incubated for 30 min with a rat anti-BrdU antibody (Oxford Biotechnology, OBT0030S) and revealed with a goat anti-rat IgG coupled with FITC fluorochrome (Southern Biotech, 3010-02). Cells were stained with propidium iodide (PI, 25 μg/ml, Invitrogen, P3566) and cytofluorometric analyses were performed.

RNA preparation and RT-Q-PCR. Total RNA was isolated from HCT116-TP53KO-EV and -MAPK14-CA cells using the RNeasy® mini Kit (Qiagen, 74104) with an additional DNase digestion step (Qiagen, 79254). RNA was quantified by UV spectroscopy. Total RNA (1 μg) was reverse transcribed using the SuperScript III reverse transcriptase (Invitrogen, 1808004). Real-time quantitative PCR was performed using the LC480 (Roche Diagnostics) according to the manufacturer's instruction. The amplification specificity was verified by using the melting curve analysis. Real-time PCR values were determined by reference to a standard curve that was generated by real-time PCR amplification of a serially diluted cDNA sample using primers specific for *CDKN1A*, *ATG5*, *ATG7* and Hypoxanthine Phosphorybosyl Transferase (*HPRT*). The quantification data were normalized to the amplification data for the reference gene *HPRT*.

Apoptosis assay. Cells were seeded in 25 cm^2 flasks (10^5 cells/flask). After 48 h, they were labeled with fluorescein isothiocyanate (FITC)-labeled Annexin V and 7AAD (Coulter, PN IM3614) to determine the number of apoptotic cells.

siRNA and transfection procedures. siRNA oligonucleotides targeting *ATG5*, *ATG7* and control non-targeting constructs (siCT) (SR-CL000-005) were obtained from Eurogentec. Transfections were performed using Oligofectamine (Invitrogen, 12252011) according to the manufacturer's instructions. Briefly, 2×10^5 cells were plated in each well of a 6-well plate and incubated overnight. A mixture of 3 μg siRNA and Oligofectamine diluted in OptiMEM (31985) was added for 6 h, followed by incubation in regular medium. Cells were harvested 96 h after siRNA transfection.

Kinase assay. The p38 kinase assay was performed using the non-radioactive p38 MAPK Assay Kit from Cell Signaling Technology (9820) with 2μg of p38 isoforms. MAPK14 mutant is p38α $^{D176A\ F327S}$, MAPK11 mutant is p38β ^{D176A}, MAPK12 mutant p38γ ^{D179A} and MAPK13 mutant p38δ ^{F324S}.

Statistical analysis. Analysis of quantitative data was performed by using the Student's t-test. Differences were considered statistically significant, when $p < 0.05$.

Disclosure of Potential Conflicts of Interest

No potential conflicts of interest were disclosed.

Acknowledgments

The authors are grateful to Chantal Cazevieille and Cécile Sanchez (*Montpellier* Rio Imaging (*MRI*) electron microscopy facility) for their technical assistance and for interpreting data concerning ultrastructural evaluation.

The authors are also grateful to the *Montpellier* Rio Imaging (*MRI*) cytometry facilities, and particularly to the technical assistance of Nadia Vié.

Funds for this research were provided by INSERM.

Supplemental Materials

Supplemental materials may be found here:
www.landesbioscience.com/journals/autophagy/article/20268

References

1. Segal NH, Saltz LB. Evolving treatment of advanced colon cancer. Annu Rev Med 2009; 60:207-19; PMID: 19630571; http://dx.doi.org/10.1146/annurev.med.60.041807.132435
2. Lièvre A, Bachet JB, Le Corre D, Boige V, Landi B, Emile JF, et al. KRAS mutation status is predictive of response to cetuximab therapy in colorectal cancer. Cancer Res 2006; 66:3992-5; PMID:16618717; http://dx.doi.org/10.1158/0008-5472.CAN-06-0191
3. Pommier Y. Topoisomerase I inhibitors: camptothecins and beyond. Nat Rev Cancer 2006; 6:789-802; PMID: 16990856; http://dx.doi.org/10.1038/nrc1977
4. Xu Y, Villalona-Calero MA. Irinotecan: mechanisms of tumor resistance and novel strategies for modulating its activity. Ann Oncol 2002; 13:1841-51; PMID: 12453851; http://dx.doi.org/10.1093/annonc/mdf337
5. Gongora C, Candeil L, Vezzio N, Copois V, Denis V, Breil C, et al. Altered expression of cell proliferation-related and interferon-stimulated genes in colon cancer cells resistant to SN38. Cancer Biol Ther 2008; 7:822-32; PMID:18340113; http://dx.doi.org/10.4161/cbt.7.6.5838
6. Paillas S, Boissière F, Bibeau F, Denouel A, Mollevi C, Causse A, et al. Targeting the p38 MAPK pathway inhibits irinotecan resistance in colon adenocarcinoma. Cancer Res 2011; 71:1041-9; PMID:21159664; http://dx.doi.org/10.1158/0008-5472.CAN-10-2726
7. Chiacchiera F, Simone C. Signal-dependent regulation of gene expression as a target for cancer treatment: inhibiting p38alpha in colorectal tumors. Cancer Lett 2008; 265:16-26; PMID:18395970; http://dx.doi.org/10.1016/j.canlet.2008.02.061

8. Yue Z, Jin S, Yang C, Levine AJ, Heintz N. Beclin 1, an autophagy gene essential for early embryonic development, is a haploinsufficient tumor suppressor. Proc Natl Acad Sci U S A 2003; 100:15077-82; PMID: 14657337; http://dx.doi.org/10.1073/pnas.2436255100
9. Liang XH, Jackson S, Seaman M, Brown K, Kempkes B, Hibshoosh H, et al. Induction of autophagy and inhibition of tumorigenesis by beclin 1. Nature 1999; 402:672-6; PMID:10604474; http://dx.doi.org/10.1038/45257
10. Avitzour M, Diskin R, Raboy B, Askari N, Engelberg D, Livnah O. Intrinsically active variants of all human p38 isoforms. FEBS J 2007; 274:963-75; PMID: 17241234; http://dx.doi.org/10.1111/j.1742-4658.2007.05644.x
11. Wang W, Chen JX, Liao R, Deng Q, Zhou JJ, Huang S, et al. Sequential activation of the MEK-extracellular signal-regulated kinase and MKK3/6-p38 mitogen-activated protein kinase pathways mediates oncogenic ras-induced premature senescence. Mol Cell Biol 2002; 22:3389-403; PMID:11971971; http://dx.doi.org/10.1128/MCB.22.10.3389-3403.2002
12. Haq R, Brenton JD, Takahashi M, Finan D, Finkielsztein A, Damaraju S, et al. Constitutive p38HOG mitogen-activated protein kinase activation induces permanent cell cycle arrest and senescence. Cancer Res 2002; 62:5076-82; PMID:12208764
13. Bulavin DV, Saito S, Hollander MC, Sakaguchi K, Anderson CW, Appella E, et al. Phosphorylation of human p53 by p38 kinase coordinates N-terminal phosphorylation and apoptosis in response to UV radiation. EMBO J 1999; 18:6845-54; PMID: 10581258; http://dx.doi.org/10.1093/emboj/18.23.6845
14. Weng MS, Ho YS, Lin JK. Chrysin induces G1 phase cell cycle arrest in C6 glioma cells through inducing p21Waf1/Cip1 expression: involvement of p38 mitogen-activated protein kinase. Biochem Pharmacol 2005; 69:1815-27; PMID:15869744; http://dx.doi.org/10.1016/j.bcp.2005.03.011
15. Klionsky DJ, Abeliovich H, Agostinis P, Agrawal DK, Aliev G, Askew DS, et al. Guidelines for the use and interpretation of assays for monitoring autophagy in higher eukaryotes. Autophagy 2008; 4:151-75; PMID: 18188003
16. Bulavin DV, Amundson SA, Fornace AJ. p38 and Chk1 kinases: different conductors for the G(2)/M checkpoint symphony. Curr Opin Genet Dev 2002; 12:92-7; PMID:11790561; http://dx.doi.org/10.1016/S0959-437X(01)00270-2
17. Kim GY, Mercer SE, Ewton DZ, Yan Z, Jin K, Friedman E. The stress-activated protein kinases p38 alpha and JNK1 stabilize p21(Cip1) by phosphorylation. J Biol Chem 2002; 277:29792-802; PMID:12058028; http://dx.doi.org/10.1074/jbc.M201299200
18. Tang G, Yue Z, Talloczy Z, Hagemann T, Cho W, Messing A, et al. Autophagy induced by Alexander disease-mutant GFAP accumulation is regulated by p38/MAPK and mTOR signaling pathways. Hum Mol Genet 2008; 17:1540-55; PMID:18276609; http://dx.doi.org/10.1093/hmg/ddn042
19. Cui Q, Tashiro SI, Onodera S, Minami M, Ikejima T. Oridonin induced autophagy in human cervical carcinoma HeLa cells through Ras, JNK, and P38 regulation. J Pharmacol Sci 2007; 105:317-25; PMID: 18094523; http://dx.doi.org/10.1254/jphs.FP0070336
20. Comes F, Matrone A, Lastella P, Nico B, Susca FC, Bagnulo R, et al. A novel cell type-specific role of p38alpha in the control of autophagy and cell death in colorectal cancer cells. Cell Death Differ 2007; 14:693-702; PMID:17159917; http://dx.doi.org/10.1038/sj.cdd.4402076
21. Webber JL, Tooze SA. Coordinated regulation of autophagy by p38alpha MAPK through mAtg9 and p38IP. EMBO J 2010; 29:27-40; PMID:19893488; http://dx.doi.org/10.1038/emboj.2009.321
22. Abedin MJ, Wang D, McDonnell MA, Lehmann U, Kelekar A. Autophagy delays apoptotic death in breast cancer cells following DNA damage. Cell Death Differ 2007; 14:500-10; PMID:16990848; http://dx.doi.org/10.1038/sj.cdd.4402039
23. Li J, Hou N, Faried A, Tsutsumi S, Kuwano H. Inhibition of autophagy augments 5-fluorouracil chemotherapy in human colon cancer in vitro and in vivo model. Eur J Cancer 2010; 46:1900-9; PMID:20231086; http://dx.doi.org/10.1016/j.ejca.2010.02.021
24. Tasdemir E, Maiuri MC, Galluzzi L, Vitale I, Djavaheri-Mergny M, D'Amelio M, et al. Regulation of autophagy by cytoplasmic p53. Nat Cell Biol 2008; 10:676-87; PMID:18454141; http://dx.doi.org/10.1038/ncb1730
25. Kondo Y, Kanzawa T, Sawaya R, Kondo S. The role of autophagy in cancer development and response to therapy. Nat Rev Cancer 2005; 5:726-34; PMID: 16148885; http://dx.doi.org/10.1038/nrc1692
26. Dimri GP, Lee X, Basile G, Acosta M, Scott G, Roskelley C, et al. A biomarker that identifies senescent human cells in culture and in aging skin in vivo. Proc Natl Acad Sci U S A 1995; 92:9363-7; PMID: 7568133; http://dx.doi.org/10.1073/pnas.92.20.9363